# Transcriptional response of kidney tissue after $^{177}$Lu-octreotate administration in mice

Emil Schüler [a],*, Nils Rudqvist [a], Toshima Z. Parris [b], Britta Langen [a], Khalil Helou [b], Eva Forssell-Aronsson [a]

[a] Department of Radiation Physics, Institute of Clinical Sciences, Sahlgrenska Cancer Center, Sahlgrenska Academy at the University of Gothenburg, Sahlgrenska University Hospital, Gothenburg, Sweden
[b] Department of Oncology, Institute of Clinical Sciences, Sahlgrenska Cancer Center, Sahlgrenska Academy at the University of Gothenburg, Sahlgrenska University Hospital, Gothenburg, Sweden

## ARTICLE INFO

## ABSTRACT

*Introduction:* The kidneys are one of the main dose limiting organs in $^{177}$Lu-octreotate therapy of neuroendocrine tumors. Therefore, biomarkers for radiation damage would be of great importance in this type of therapy. The purpose of this study was to investigate the absorbed dose dependency on early transcriptional changes in the kidneys from $^{177}$Lu-octreotate exposure.
*Methods:* Female Balb/c nude mice were i.v. injected with 1.3, 3.6, 14, 45 or 140 MBq $^{177}$Lu-octreotate. The animals were killed 24 h after injection followed by excision of the kidneys. The absorbed dose to the kidneys ranged between 0.13 and 13 Gy. Total RNA was extracted from separated renal tissue samples, and applied to Illumina MouseRef-8 Whole-Genome Expression Beadchips to identify regulated transcripts after irradiation. Nexus Expression 2.0 and Gene Ontology terms were used for data processing and to determine affected biological processes.
*Results:* Distinct transcriptional responses were observed following $^{177}$Lu-octreotate administration. A higher number of differentially expressed transcripts were observed in the kidney medulla (480) compared to cortex (281). In addition, 39 transcripts were regulated at all absorbed dose levels in the medulla, compared to 32 in the cortex. Three biological processes in the cortex and five in the medulla were also shared by all absorbed dose levels. Strong association to metabolism was found among the affected processes in both tissues. Furthermore, an association with cellular and developmental processes was prominent in kidney medulla, while transport and immune response were prominent in kidney cortex.
*Conclusion:* Specific biological and dose-dependent responses were observed in both tissues. The number of affected transcripts and biological processes revealed distinct response differences between the absorbed doses delivered to the tissues.

© 2014 Elsevier Inc. Open access under CC BY-NC-ND license.

## 1. Introduction

Therapy using radiolabeled somatostatin analogs has become a novel approach for treatment of somatostatin receptor-overexpressing neuroendocrine (NE) tumors. Successful results have been shown in tumor regression, increased overall survival, and improved quality of life for patients with different types of NE tumors [1,2].

Uptake of radiolabeled somatostatin analogs in normal tissues is generally lower than in tumor tissue [3,4]. The highest normal tissue uptake takes place in the kidneys via, e.g., active reabsorption of radiolabeled octreotate in the proximal tubule of the nephron [5–8].

Uptake values of 5–7.7%IA/g have been reported in mice 24 h after injection of $^{177}$Lu-octreotate, while lower values have been reported in humans (after infusion of basic amino acids) [9–11]. Despite blocking of kidney uptake, the kidneys are still one of the main dose limiting organs when patients undergo therapy with $^{177}$Lu-octreotate [12]. The routinely used kidney absorbed dose limit is taken from experience from external beam radiation therapy with nephropathy as endpoint [13]. However, data from external beam therapy cannot be directly translated to radionuclide therapy, due to the much lower dose rate, the continuous irradiation, and the inhomogeneous dose distribution within the organs and body in radionuclide therapy [14]. Since there is still limited knowledge on normal tissue effects after radionuclide therapy, it is hard to define tolerance doses to the kidneys for this application. Animal studies have shown nephrotoxicity after injection with 90 MBq and 280–560 MBq $^{177}$Lu-octreotate in mice and rats, respectively [8,15]. Furthermore, nephrotoxicity has also been shown clinically (early

* Corresponding author at: Department of Radiation Physics, Sahlgrenska University Hospital, SE-413 45 Gothenburg, Sweden. Tel.: +46 31 3429695.
  E-mail address: emil.schuler@gu.se (E. Schüler).

^{90}Y-DOTATOC studies), with renal function loss and end-stage renal disease [12,14,16,17]. The latency times of acute and chronic radiation-induced nephropathy vary. Acute nephropathy may be induced after 6–12 months, while chronic nephropathy may be induced up to 5 years after therapy. Therefore, it is important to monitor renal function over long time periods after therapy [14].

There is a need for a better understanding of the biological response following irradiation of the kidneys with ^{177}Lu-octreotate, to minimize side effects and, if possible, to enlarge the therapeutic window and success rate [18]. Gene expression analysis using microarray technology has the ability to provide a comprehensive view of the biological effects after exposure to ionizing radiation. This technique allows for a direct whole genome, transcriptome, and proteome investigation of the cellular responses to radiation. Microarray analysis has been employed successfully to elucidate the effects on normal tissues and to develop a deeper understanding of the potential molecular targets and biological events initiated in irradiated tissue [19,20]. Nevertheless, only a few studies using global gene expression analysis of irradiated kidneys have been published, which predominantly used external irradiation of animal models [19–21]. To our knowledge there are only two reports on global gene expression studies following internal irradiation of the kidneys [22,23]. These studies showed a clear response of the kidneys from very low absorbed doses (0.20–3.5 mGy) of ^{131}I and 0.24–160 mGy of [211]At at 24 h after injection [22,23]. However, further studies are needed to better understand the biological response of radiation as a basis for defining possible clinically useful biomarkers for early radiation nephrotoxicity.

The aim of this study was to investigate early transcriptional response in kidney cortex and medulla after i.v. injection of different amounts of ^{177}Lu-octreotate in mice.

## 2. Materials and Methods

### 2.1. Radiopharmaceutical

[177]LuCl$_3$ and DOTA-Tyr[3]-octreotate were acquired from I.D.B. Holland (I.D.B. Holland BV, Baarle-Nassau, Netherlands). Preparation and radiolabeling were conducted according to the manufacturer's instructions. Instant thin layer chromatography (ITLC) revealed that the fraction of peptide bound ^{177}Lu was higher than 99%. The ^{177}Lu-octreotate stock solution was diluted to the final activity concentrations with saline solution.

Before and after administration, the ^{177}Lu activity in the syringes was measured with a well-type ionization chamber (CRC-15R; Capintec, IA, USA) to determine the injected activity in each animal.

### 2.2. Animals

Female BALB/c nude mice (Charles River, Salzfeld, Germany) were divided into six groups with three animals in each and were kept under normal nutritional conditions. Five groups were i.v. injected with 1.3, 3.6, 14, 45, and 140 MBq ^{177}Lu-octreotate (0.04 µg octreotate/MBq), while the control group was i.v. injected with saline solution. The experimental protocol was approved by the Ethical Committee on Animal Experiments in Gothenburg, Sweden.

Twenty-four hours after injection the animals were killed by cardiac puncture under anesthesia (pentobarbitalnatrium, APL, Sweden) and the kidneys were surgically removed. One kidney from each animal was immediately flash frozen in liquid nitrogen and stored at −80 °C until analysis. The remaining kidney was weighed and the ^{177}Lu activity was measured with a gamma counter (Wallac 1480 Wizard, Wallac Oy, Turku, Finland). The gamma counter was calibrated against the ionization chamber. Corrections were done for background signal and dead time effects.

### 2.3. Dosimetry

Estimations of the absorbed dose to the kidneys were made according to the Medical Internal Radiation Dose (MIRD) formalism [24]:

$$\overline{D}_{Kidney} = \tilde{A}_{Kidney} \sum n_i E_i \phi_i / m_{Kidney} ,$$

where $\tilde{A}_{Kidney}$ is the cumulated activity during the first 24 h after injection

$$\tilde{A}_{Kidney} = \int_0^{24h} A_{kidney}(t)dt ,$$

the product $n_i E_i$ is the average energy emitted by electrons per decay, $\phi_i$ is the absorbed fraction and $m_{Kidney}$ is the mass of the kidney investigated. Values for $\tilde{A}_{tissue}$ were estimated based on previously published biodistribution data of ^{177}Lu-octreotate in nude mice together with the activity concentration measurements of the removed kidneys in the present study [10]. A mono-exponential curve was fitted to the time-activity concentration data obtained. The integral of the fitted equation was calculated for 0–24 h to estimate the cumulated activity. The absorbed fraction, $\phi_i$, was assumed to be 0.93 [25]. Only the contribution from the electrons was included in the dosimetric calculations. The absorbed dose was determined for the whole kidney.

### 2.4. RNA extraction and analysis

The flash-frozen kidneys were dissected into cortical and medullary tissues and homogenized using the Mikro-Dismembrator S ball mill (Sartorius Stedim Biotech). Total RNA was extracted using the RNeasy Lipid Tissue Mini Kit (Qiagen), according to the manufacturer´s instructions. RNA Integrity Number (RIN) values were retrieved using RNA 6000 Nano LabChip Kit with Agilent 2100 Bioanalyzer (Agilent Technologies) and samples with RIN values above 6.0 were accepted for further analysis (lowest RIN value in the present study was 6.6 with a mean value of 8.2).

Processing of the RNA samples was conducted at the Swegene Center for Integrative Biology at Lund University (SCIBLU). MouseRef-8 Whole-Genome Expression Beadchips (Illumina), containing 25,435 probes were used for hybridization. Image acquisition and subsequent analysis were performed with Illumina BeadArray Reader scanner and BeadScan 3.5.31.17122 image analysis software, respectively.

### 2.5. Data processing and statistical analysis

Data preprocessing and quantile normalization of raw signal intensities were conducted through the use of the web-based BioArray Software Environment (BASE) system. Nexus Expression 2.0 (BioDiscovery) was used for further analysis with log2-transformed, normalized expression values and a variance filter.

To determine differentially expressed transcripts and to control the false discovery rate, the Benjamini–Hochberg method was used [26]. A p-adjusted value of 0.01 and a fold change of at least 1.5 (up- or down-regulation) were considered statistically significant. Generated gene expression profiles are displayed at NCBI´s Gene Expression Omnibus (GEO accession number GSE44762).

Gene Ontology (GO) terms were used to determine affected biological processes (the biochemical reactions, known to be regulated by the genes whose expression was affected) from differentially regulated gene sets using two separate approaches. First, GO terms were determined in Nexus Expression, employing a $p$ value cutoff of 0.05. However, 40% of the filtered Illumina transcripts are not assigned to a known biological process. Therefore, a complete listing of annotated genes was compiled for differentially regulated transcripts using the Gene Ontology website (http://www.geneontology.org/). Using this list, transcripts with a log$_2$-ratio

above 2 for either positive or negative regulation, were then categorized into eight main GO categories and further subcategories: DNA integrity, cell communication, cell cycle and differentiation, cellular integrity, gene expression integrity, metabolism, organismic response, and stress response.

## 2.6. Quantitative real-time PCR (QPCR)

To verify the microarray results, nine significant differentially expressed genes detected in both renal tissues at all absorbed dose levels (*Angpti4, Cyp24a1, Dnase1, Gldc, Hmgcs2, Igfbp4, S100a8, Slc25a20,* and *Slc25a25*) were selected and scrutinized using the quantitative real-time polymerase chain reaction (QPCR) assay. Another three constitutive genes (*B2m, Gusb,* and *Ywhaz*), which showed homogenous expression through the microarray analysis were used for normalization. Commercially available validated Taq-Man® Gene Expression Assays were obtained from Applied Biosystems (Carlsbad, CA, USA). For each specimen cDNA was synthesized from 1 μg total RNA (the same RNA extraction as in the microarray experiments) using SuperScript™ III First-Strand Synthesis SuperMix for qRT-PCR (Invitrogen, Carlsbad, CA, USA) according to the manufacturer´s protocol. The standard curve method was used for quantification and the geometric mean of the three endogenous controls (*B2m, Gusb,* and *Ywhaz*) was used for normalization of the samples. The Pearson correlation coefficient was used to calculate the correlation between the microarray and the QPCR results.

## 3. Results

### 3.1. Dosimetry

The absorbed doses to the kidneys were estimated to 0.13, 0.34, 1.3, 4.3, and 13 Gy during 24 h after injection of 1.3, 3.6, 14, 45, and 140 MBq $^{177}$Lu-octreotate, respectively. The absorbed dose estimated to infinity time would correspond to 0.31, 0.85, 3.3, 11, and 32 Gy, respectively.

### 3.2. Differentially regulated transcripts

A clear biological response at the transcriptional level was seen in both kidney cortex and medulla following administration of $^{177}$Lu-octreotate. In total, 281 and 480 differentially regulated transcripts were detected in the kidney cortex and medulla, respectively.

In kidney cortex, the number of regulated transcripts varied with absorbed dose. The highest number of regulated transcripts compared to control was found at 4.3 Gy (180 transcripts), with a reduction in the number of regulated transcripts at both higher and lower absorbed doses (Table 1). When comparing differences and similarities between exposed groups, few common transcripts were seen between 1.3 and 13 Gy, with only 6 transcripts. With the exception of the 80 differentially expressed transcripts between 4.3 and 13 Gy, the number of differentially expressed transcripts increased with increased difference in absorbed dose.

The fraction of dose-specific regulated transcripts in the kidney cortex was around 30% for 0.13, 4.3, and 13 Gy, while for 0.34 and 1.3 Gy this number was reduced to 6% and 12%, respectively (Table 2).

In kidney medulla, the highest number of regulated transcripts was found at 1.3 Gy (348 regulated transcripts). For both higher and lower absorbed doses, the number of regulated transcripts was clearly reduced, e.g. 147 at 0.34 Gy and 205 at 4.3 Gy. At the other dose levels, 143 (0.13 Gy) and 130 (13 Gy) regulated transcripts were detected (Table 1). In the comparison of the inter-dose response, a prominent difference could be seen between 0.34 and 1.3 Gy, 1.3 and 13 Gy, as well as between 1.3 and 4.3 Gy with 422, 364, and 282 differentially expressed transcripts, respectively, while the difference in response between 0.13 and 0.34 Gy was weak (27 differentially regulated

Table 1
Number of differentially regulated transcripts in the kidney cortex and medulla.

| Kidney cortex | | Control | | 0.13 Gy | | 0.34 Gy | | 1.3 Gy | | 4.3 Gy | |
|---|---|---|---|---|---|---|---|---|---|---|---|
| *Absorbed dose* | 0.13 Gy | 98 | ↑ 53 | | | | | | | | |
| | | | ↓ 45 | | | | | | | | |
| | 0.34 Gy | 83 | ↑ 29 | 24 | ↑ 3 | | | | | | |
| | | | ↓ 54 | | ↓ 21 | | | | | | |
| | 1.3 Gy | 113 | ↑ 43 | 16 | ↑ 5 | 10 | ↑ 10 | | | | |
| | | | ↓ 70 | | ↓ 11 | | ↓ 0 | | | | |
| | 4.3 Gy | 180 | ↑ 83 | 51 | ↑ 28 | 40 | ↑ 35 | 35 | ↑ 16 | | |
| | | | ↓ 97 | | ↓ 23 | | ↓ 5 | | ↓ 19 | | |
| | 13 Gy | 134 | ↑ 75 | 100 | ↑ 51 | 55 | ↑ 47 | 6 | ↑ 1 | 80 | ↑ 33 |
| | | | ↓ 59 | | ↓ 49 | | ↓ 8 | | ↓ 5 | | ↓ 47 |
| **Kidney medulla** | | | | | | | | | | | |
| *Absorbed dose* | 0.13 Gy | 143 | ↑ 73 | | | | | | | | |
| | | | ↓ 70 | | | | | | | | |
| | 0.34 Gy | 147 | ↑ 63 | 27 | ↑ 6 | | | | | | |
| | | | ↓ 84 | | ↓ 21 | | | | | | |
| | 1.3 Gy | 348 | ↑ 215 | 297 | ↑ 259 | 422 | ↑ 387 | | | | |
| | | | ↓ 133 | | ↓ 38 | | ↓ 35 | | | | |
| | 4.3 Gy | 205 | ↑ 84 | 78 | ↑ 33 | 36 | ↑ 29 | 282 | ↑ 24 | | |
| | | | ↓ 121 | | ↓ 45 | | ↓ 7 | | ↓ 258 | | |
| | 13 Gy | 130 | ↑ 68 | 131 | ↑ 69 | 185 | ↑ 115 | 364 | ↑ 69 | 84 | ↑ 61 |
| | | | ↓ 62 | | ↓ 62 | | ↓ 70 | | ↓ 295 | | ↓ 23 |

Number of regulated transcripts in kidney cortex and medulla is shown for each absorbed dose, compared to either non-irradiated controls or a lower dose level. The number of up/down regulated transcripts is indicated in green/red.

transcripts). In addition, no increase in number of differentially regulated transcripts could be seen with increasing difference in absorbed dose (Table 1). The increased number of regulated transcripts at 1.3 Gy resulted in a higher fraction of unique transcripts (47%) regulated at this specific dose level (Table 2).

In total, 32 and 39 transcripts were regulated in all irradiated groups for kidney cortex and medulla, respectively (Table 3). Among these, 22 transcripts were shared by both tissues. Of these 49 transcripts, the UniGene repository showed that 69% and 72% in kidney cortex and medulla, respectively, are normally expressed in the mouse kidney, while three transcripts could not be found in the repository. The regulation profiles vs. injected activity showed large variations between the different transcripts. In general, the expression variation of the majority of the analyzed transcripts was relatively similar irrespective of absorbed dose. The only obvious monotonous dose–response relationship was found for *Hmgcs2*, with very high up-regulation after exposure to the lowest absorbed dose, and decreasing expression with increased absorbed dose for both kidney cortex and medulla. Similar profiles were also found for *Igfbp4* in kidney cortex. *Angptl4* (angiopoietin-like 4) showed a constant expression in both cortex and medulla at all but the highest absorbed dose, where a reduced expression was found. *Cyp24a1* (Cytochrome P450) showed a very strong expression in the 14 MBq group in both kidney cortex and medulla, with reduced expression at the other dose levels investigated.

Transcripts with log$_2$-ratio above 2, for either positive or negative regulation, are presented in Table 4. Few transcripts had log$_2$-ratios above 2: 21 transcripts in the cortex and 13 in the medulla. In both tissues, enriched transcripts were generally involved in cell cycle and differentiation at the highest dose level (13 Gy), stress responses at the intermediate dose levels (1.3 and 4.3 Gy), and cellular integrity at the lowest absorbed dose level (0.13 Gy). In addition, regulated transcripts related to metabolism were seen at all but the highest dose levels. No genes with regulated expression above/below this threshold (log$_2$-ratio > 2 or < 0.5, respectively) were found to be associated with gene expression integrity, cell communication, or organismic regulation.

Table 2
Distribution of common and dose-specific differentially regulated transcripts.

| | Kidney cortex | | | | | | Kidney medulla | | | | | |
|---|---|---|---|---|---|---|---|---|---|---|---|---|
| | 0.13 Gy (98) | 0.34 Gy (83) | 1.3 Gy (113) | 4.3 Gy (180) | 13 Gy (134) | No. | 0.13 Gy (143) | 0.34 Gy (147) | 1.3 Gy (348) | 4.3 Gy (205) | 13 Gy (130) | No. |
| | 27.6% | | | | | 27 | 14.0% | | | | | 20 |
| | | 6.0% | | | | 5 | | 15.0% | | | | 22 |
| | | | 12.4% | | | 14 | | | 46.8% | | | 163 |
| | | | | 26.7% | | 48 | | | | 8.8% | | 18 |
| | | | | | 30.6% | 41 | | | | | 14.6% | 19 |
| | 1.0% | 1.2% | | | | 1 | 2.8% | 2.7% | | | | 4 |
| | 7.1% | | 6.2% | | | 7 | 9.8% | | 4.0% | | | 14 |
| | 5.1% | | | 2.8% | | 5 | 4.2% | | | 2.9% | | 6 |
| | 1.0% | | | | 0.7% | 1 | 1.4% | | | | 1.5% | 2 |
| | | 0.0% | 0.0% | | | 0 | | 4.8% | 2.0% | | | 7 |
| | | 6.0% | | 2.8% | | 5 | | 12.9% | | 9.3% | | 19 |
| | | 3.6% | | | 2.2% | 3 | | 0.0% | | | 0.0% | 0 |
| | | | 9.7% | 6.1% | | 11 | | | 8.0% | 13.7% | | 28 |
| | | | 0.0% | | 0.0% | 0 | | | 2.3% | | 6.2% | 8 |
| | | | | 9.4% | 12.7% | 17 | | | | 7.3% | 11.5% | 15 |
| | 0.0% | 0.0% | 0.0% | | | 0 | 7.7% | 7.5% | 3.2% | | | 11 |
| | 6.1% | 7.2% | | 3.3% | | 6 | 4.2% | 4.1% | | 2.9% | | 6 |
| | 0.0% | 0.0% | | | 0.0% | 0 | 0.0% | 0.0% | | | 0.0% | 0 |
| | 4.1% | | 3.5% | 2.2% | | 4 | 8.4% | | 3.4% | 5.9% | | 12 |
| | 2.0% | 1.8% | | | 1.5% | 2 | 3.5% | | 1.4% | | 3.8% | 5 |
| | 2.0% | | | 1.1% | 1.5% | 2 | 0.0% | | | 0.0% | 0.0% | 0 |
| | | 13.3% | 9.7% | 6.1% | | 11 | | 3.4% | 1.4% | 2.4% | | 5 |
| | | 0.0% | 0.0% | | 0.0% | 0 | | 0.0% | 0.0% | | 0.0% | 0 |
| | | 3.6% | | 1.7% | 2.2% | 3 | | 0.7% | | 0.5% | 0.8% | 1 |
| | | | 13.3% | 8.3% | 11.2% | 15 | | | 4.3% | 7.3% | 11.5% | 15 |
| | 3.1% | 3.6% | 2.7% | 1.7% | | 3 | 10.5% | 10.2% | 4.3% | 7.3% | | 15 |
| | 0.0% | 0.0% | 0.0% | | 0.0% | 0 | 0.0% | 0.0% | 0.0% | | 0.0% | 0 |
| | 4.1% | 4.8% | | 2.2% | 3.0% | 4 | 0.0% | 0.0% | | 0.0% | 0.0% | 0 |
| | 4.1% | | 3.5% | 2.2% | 3.0% | 4 | 5.6% | | 2.3% | 3.9% | 6.2% | 8 |
| | | 12.0% | 8.8% | 5.6% | 7.5% | 10 | | 11.6% | 4.9% | 8.3% | 13.1% | 17 |
| | 32.7% | 38.6% | 28.3% | 17.8% | 23.9% | 32 | 28.0% | 27.2% | 11.5% | 19.5% | 30.8% | 40 |

The total number of uniquely (rows 1–5) or commonly (rows 6–31) regulated transcripts for one or more absorbed doses is given in columns 6 and 12 for the kidney cortex and medulla. The distribution of differentially expressed transcripts per absorbed dose is given as percentage of the total number of regulated transcripts per absorbed dose level. The total number of regulated transcripts per dose level compared to controls is given in parenthesis. The percentage of scored transcripts is color coded according to strength of regulation.

The expression profiles between the groups were verified for both tissues at all dose levels using QPCR. The two methods (microarray and QPCR) showed strong correlation ($r > 0.85$) for all genes tested (*Angpti4, Cyp24a1, Dnase1, Gldc, Hmgcs2, Igfbp4, S100a8, Slc25a20,* and *Slc25a25*).

### 3.3. Affected biological processes

A total of 91 biological processes were affected by the administration of ^{177}Lu-octreotate in both kidney cortex and medulla, but the type of processes as well as the occurrence at each absorbed dose level differed (Figs. 1 & 2, Supplementary Table S1 & S2). Kidney medulla had a higher number of biological processes affected at the highest absorbed dose compared to kidney cortex (32 vs. 22). At 1.3 and 4.3 Gy, kidney cortex had a higher number of affected biological processes compared to kidney medulla (40 and 41 vs. 23 and 34, respectively). A similar number of affected biological processes were found for the two tissues at the two lowest dose levels.

In both tissues, the affected biological processes were strongly associated with metabolic processes at all dose levels, with the strongest association found at the lowest dose level (0.13 Gy) (Figs. 1 & 2, Supplementary Table S1 & S2). The association with metabolic processes was lower at the higher absorbed doses as a result of a reduction of processes associated with the metabolism of proteins/ amino acids and lipids/fatty acids. Regulation of carbohydrate metabolism included a heterogeneous mixture of various biological processes, but the total number of regulated processes remained on a similar level at all absorbed doses.

In both tissues, immune response was the predominantly affected subcategory of stress responses. The highest impact was found at 1.3

and 4.3 Gy with examples such as cellular defense response, positive regulation of immune response and positive regulation of T cell differentiation. No biological processes associated with DNA integrity were observed for either tissue and an effect on gene expression integrity was only observed in the kidney medulla. (Figs. 1A & 2A, Supplementary Table S1 & S2).

Immune response, as a specific biological process, was the only process affected at all absorbed doses and in both tissues. However, the strength of the response differed between the tissues. In kidney cortex and medulla, 23 and 34 genes were regulated at one or more dose levels, respectively. In medulla, a higher number of regulated genes associated with immune response were found at all dose levels, compared to cortex (6 vs 2). The two regulated genes (*Serpina3g* and *Tgtp*) in the cortex were also regulated in medulla. *Serpina3g* is associated with apoptosis, regulation of proteolysis, and response to cytokine stimulus, whereas *Tgtp* is associated with cellular response to interferon-beta.

## 4. Discussion

Normal tissue exposure to radiation is inevitable during radionuclide therapy. Consequently, radiation-induced normal tissue effects set the limit for the radionuclide activity that can safely be administered, and hence the absorbed dose to tumor tissue. $^{177}$Lu-octreotate therapy has shown great promise in the treatment of neuroendocrine tumors. One of the main critical organs for $^{177}$Lu-octreotate therapy of neuroendocrine tumors is the kidneys. In the present study, the transcriptional effects of $^{177}$Lu-octreotate irradiation on cortical and medullary kidney tissues were investigated in non-tumor bearing mice in an attempt to increase our understanding of the early response in kidneys during this type of therapy. These effects were studied using gene expression microarray analysis, where the entire mouse transcriptome was investigated to identify differentially expressed transcripts and affected biological processes. Strong biological response, both general and tissue-specific, was seen in both kidney cortex and medulla.

There are large individual variations in absorbed dose to the kidneys per fraction in patients undergoing $^{177}$Lu-octreotate therapy, with values of 0.33–2.4 Gy/GBq (corresponding to 2.4–17 Gy per fraction) [11]. In order to have clinically relevant absorbed doses in the present study, the injected activities of 14 and 45 MBq, corresponding to absorbed doses of 3.3 and 11 Gy when estimated to infinity, were chosen. The highest absorbed dose in the present study was 13 Gy delivered over 24 h. However, the estimated absorbed dose to infinity time would correspond to 32 Gy, where the risk of nephrotoxicity would be present [13]. Finding early biomarkers for kidney toxicity is of highest concern to optimize individualized patient treatment. This study represents one step towards finding novel early biomarkers for kidney toxicity, but also presents data that may lead to a better understanding of the mechanisms behind radiation induced effects on kidney tissue. In future studies, the early transcriptional effects should be compared to those of later time points, as well as functional and morphological effects, in order to find possible correlation between early indicators/biomarkers and late toxicity.

The absorbed dose calculations were carried out using activity concentration measurements of the kidneys in the present study and previously published data [10]. The mice in the biodistribution study were tumor bearing and it was assumed that the presence of tumors did not influence the $^{177}$Lu concentration in the kidneys due to limited uptake in tumor tissue (0.23%IA/g in tumor vs. 6.2%IA/g in kidney at 24 h). Furthermore, the uptake in kidney tissue is highly heterogeneous, with highest accumulation taking place in the kidney cortex, whereas the concentration in the outer medulla corresponds to 50%–60% of the cortical activity [27]. In addition, the cortical uptake is also heterogeneous, with the highest accumulation taking place in the proximal tubules, with very low amounts detected in the distal tubules and the glomeruli [27–29]. However, due to the small size of the mouse kidney, together with the relatively long range of the beta particles emitted by $^{177}$Lu (maximum range in water: 1.6 mm), a relatively homogenous dose distribution was assumed. Therefore, the differences in the transcriptional variations of the two tissues (kidney cortex and medulla) observed in the present study are assumed to depend on the differences of the analyzed tissues, and not on possible differences in the radiation parameters. A previous study using $^{131}$I detected differences in the response between kidney cortex and medulla [22]. Similar tendencies as in the present investigation were observed with increased number of regulated transcripts in kidney medulla as compared to kidney cortex. Furthermore, the detected response in the present study is considered to depend on the properties of the irradiation, and not on the somatostatin analogue itself. We have previously found that only minor transcriptional variations are induced in the kidneys 24 h after administration of octreotate (Schüler et al., unpublished data).

A comparison of the detected differentially regulated transcripts in the kidney cortex and medulla showed both tissue-specific and common regulations. However, the response in the kidney medulla at 1.3 Gy was surprisingly strong. At this dose level, the number of uniquely regulated transcripts was 8 times higher than what was observed at both higher and lower absorbed doses (163 vs. 18–22 uniquely regulated transcripts). In addition, among the uniquely regulated transcripts identified at 1.3 Gy, 82% were up-regulated, which accounts for the substantial differences seen between the kidney cortex and medulla at this dose level. The reasons for this deviation specifically at 1.3 Gy is not known, but similar overall results have been obtained in the thyroid in vivo after 1.4 Gy exposure to $^{211}$At [30]. In that study, we stipulated that the biological response does not only vary in magnitude but also in the fundamental response at various absorbed doses. Additionally, we suggested that a strong response was observed when the absorbed dose is high enough to impose severe cellular damage but low enough to allow repair. Since $^{211}$At is an alpha emitter with high RBE, a similar effect for $^{177}$Lu would be expected at higher absorbed doses. However, a direct comparison is not possible due to the differences in tissue type and radionuclide properties.

Significant differences among affected biological processes were seen between higher and lower absorbed doses, e.g. increased association with stress response and a reduced association with metabolic processes with increasing absorbed dose. However, this trend is reduced when assessing the number of uniquely regulated genes per biological process and absorbed dose. A higher number of stress response associated genes were detected at most absorbed doses compared to those associated with metabolism. Also, the difference seen between metabolism compared to the other categories, e.g. cell communication, cell cycle and differentiation, cellular integrity, and gene expression integrity, was lower when assessing only the number of uniquely regulated genes, as opposite to the number of affected biological processes. However, the impact of this difference on these higher levels of cellular functions is unknown and larger studies with larger number of time points and inclusion of functional data is needed in order to elucidate these results.

One of the main molecular lesions induced by ionizing radiation is DNA damage. While processes associated with cell cycle regulation and cell death were affected in this study, indicating DNA damage, no processes were found to be associated with maintenance of DNA integrity and only a few processes were associated with gene expression integrity. This could be explained by inadequate information or artifacts in the ontology. However, while it is known from in vitro studies that the transcriptional response after genotoxic stress affects processes associated with cell cycle regulation and DNA repair, a more general response is also usually observed with modulation of cell-death pathways, energy metabolism, cell–cell communication and RNA processing, making the response to genotoxic stress very diverse [31–33]. Furthermore,

Table 3
Regulated transcripts in common at all dose levels after ^{177}Lu-octreotate exposure in nude mice.

| Gene symbol | Kidney cortex | | | | | Kidney medulla | | | | | Normal kidney tissue expression Gene expression[a] | Description |
| | 0.13 Gy | 0.34 Gy | 1.3 Gy | 4.3 Gy | 13 Gy | 0.13 Gy | 0.34 Gy | 1.3 Gy | 4.3 Gy | 13 Gy | Mouse | |
| --- | --- | --- | --- | --- | --- | --- | --- | --- | --- | --- | --- | --- |
| Serpina3g | −1.5 | −1.6 | −1.8 | −1.6 | −1.2 | −1.7 | −1.3 | −1.7 | −1.7 | −1.4 | - | Serpin peptidase inhibitor |
| Gbp1 | −1.4 | −1.4 | −1.8 | −2.1 | −1.5 | −1.5 | −1.4 | −1.7 | −1.9 | −1.6 | - | Guanylate binding protein |
| Igtp | −1.3 | −1.6 | −2.0 | −2.1 | −1.5 | −1.5 | −1.5 | −2.1 | −2.2 | −1.7 | Yes | Interferon gamma induced GTPase |
| Ifi47 | −1.3 | −1.7 | −1.6 | −1.8 | −1.6 | −1.5 | −1.6 | −1.4 | −1.9 | −1.6 | NA | Interferon gamma inducible protein |
| LOC100048554 | −1.1 | −1.0 | −1.2 | −0.9 | −1.0 | −1.6 | −1.1 | −1.7 | −1.9 | −1.3 | NA | - |
| Gbp2 | −1.2 | −1.4 | −1.7 | −2.0 | −1.3 | −1.4 | −1.3 | −1.7 | −1.8 | −1.4 | - | Guanylate binding protein 2 |
| Tgtp | −1.3 | −1.4 | −1.6 | −1.6 | −1.5 | −1.2 | −1.3 | −1.3 | −1.6 | −1.3 | Yes | T-cell specific GTPase |
| Iigp2 | −1.1 | −1.3 | −1.5 | −1.7 | −1.3 | −1.2 | −1.3 | −1.5 | −1.6 | −1.2 | NA | Immunity-related GTPase |
| Timd2 | −1.3 | −1.3 | −1.4 | −1.6 | −1.1 | −0.9 | −1.0 | −1.4 | −1.2 | −1.0 | Yes | T-cell immunoglobulin and mucin domain containing 2 |
| Irf1 | −1.0 | −1.3 | −1.3 | −1.6 | −1.0 | −1.2 | −1.1 | −1.5 | −1.4 | −1.1 | Yes | Interferon regulatory factor 1 |
| Ciita | −1.0 | −1.1 | −1.3 | −1.4 | −1.3 | −0.9 | −1.0 | −1.1 | −1.1 | −1.1 | Yes | Class II transactivator |
| Dbp | 1.2 | 1.3 | 1.4 | 1.2 | 1.4 | 0.9 | 1.2 | 1.3 | 1.3 | 1.2 | Yes | D site albumin promoter binding protein |
| Cyp4b1 | 1.3 | 1.2 | 1.1 | 1.4 | 1.2 | 1.2 | 0.9 | 1.0 | 1.3 | 0.9 | Yes | Cytochrome P450, family 4, subfamily B, polypeptide 1 |
| Cyp24a1 | 1.3 | 1.6 | 2.7 | 1.9 | 1.6 | 1.2 | 1.6 | 2.6 | 1.8 | 1.3 | Yes | Cytochrome P450, family 24, subfamily A, polypeptide 1 |
| Paqr7 | 1.2 | 1.5 | 1.3 | 1.3 | 1.2 | 1.3 | 1.4 | 1.1 | 1.4 | 1.0 | Yes | Progestin and adipoQ receptor family member 7 |
| Acaa2 | 1.4 | 1.1 | 1.2 | 1.1 | 1.1 | 1.1 | 1.0 | 1.0 | 1.1 | 1.0 | Yes | Acetyl-CoA acyltransferase 2 |
| Dnase1 | 1.4 | 1.4 | 1.4 | 1.5 | 1.1 | 1.2 | 1.3 | 1.2 | 1.3 | 0.8 | Yes | Deoxyribonuclease I |
| Slc25a20 | 1.4 | 1.3 | 1.2 | 1.1 | 0.9 | 1.2 | 1.3 | 1.1 | 0.9 | 0.8 | Yes | Solute carrier family 25 (carnitine/acylcarnitine translocase), member 20 |
| Slc25a25 | 1.7 | 1.9 | 1.9 | 1.4 | 1.2 | 1.3 | 1.4 | 1.5 | 1.2 | 1.0 | Yes | Solute carrier family 25 (mitochondrial carrier; phosphate carrier), member 25 |
| Gldc | 1.7 | 1.6 | 1.0 | 1.1 | 1.1 | 1.6 | 1.5 | 0.8 | 1.2 | 0.8 | Yes | Glycine dehydrogenase (decarboxylating) |
| Angptl4 | 2.2 | 1.9 | 2.3 | 2.0 | 1.5 | 2.0 | 1.8 | 1.9 | 1.8 | 1.3 | Yes | Angiopoietin-like 4 |
| Hmgcs2 | 2.7 | 2.4 | 1.9 | 1.7 | 1.3 | 2.7 | 2.5 | 1.9 | 1.7 | 1.1 | Yes | 3-hydroxy-3-methylglutaryl-CoA synthase 2 (mitochondrial) |
| Slc7a12 | −2.1 | −1.7 | −1.9 | −1.6 | −1.6 | −1.0 | – | – | – | −1.0 | Yes | Solute carrier family 7 (anionic amino acid transporter), member 12 |
| Serpina10 | −2.1 | −1.9 | −1.9 | −2.3 | −1.5 | −1.2 | – | −1.4 | −1.3 | – | – | Serpin peptidase inhibitor, clade A (alpha-1 antiproteinase, antitrypsin), member 10 |
| Havcr1 | −2.0 | −1.4 | −1.6 | −1.6 | −1.6 | −0.8 | – | −1.0 | – | −1.2 | – | Hepatitis A virus cellular receptor 1 |
| Gb p3 | −1.9 | −1.3 | −1.9 | −1.7 | −1.3 | −1.2 | – | −1.3 | −1.1 | −1.1 | Yes | Guanylate binding protein 3 |
| Slc12a1 | −1.5 | −1.5 | −1.5 | −1.4 | −1.3 | −1.1 | −1.1 | −1.2 | – | – | Yes | Solute carrier family 12 (sodium/potassium/chloride transporters), member 1 |
| Fpr2 | −1.3 | −1.3 | −1.7 | −1.2 | −1.2 | −1.2 | – | −1.4 | −1.2 | – | – | Formyl peptide receptor 2 |
| Cd274 | −1.2 | −1.2 | −1.4 | −1.4 | −1.4 | – | – | −1.1 | −1.1 | – | – | CD274 antigen |
| Ly6f | −1.0 | −1.0 | −1.3 | −1.2 | −1.0 | – | – | – | – | – | Yes | Lymphocyte antigen 6 complex, locus H |
| Ccrn4l | 0.9 | 1.4 | 1.8 | 1.9 | 1.2 | – | 0.9 | 1.4 | 1.1 | – | Yes | CCR4 carbon catabolite repression 4-like |
| Igfbp4 | 1.4 | 1.3 | 1.3 | 1.2 | 0.9 | 1.2 | 1.2 | 1.0 | – | – | Yes | Insulin-like growth factor binding protein 4 |
| Gvin1 | – | −1.6 | −1.7 | −1.8 | −1.1 | −1.1 | −1.1 | −1.5 | −1.3 | −1.0 | – | GTPase, very large interferon inducible pseudogene 1 |
| H2-Ab1 | – | −1.7 | −2.1 | −2.5 | −1.2 | −1.1 | −1.4 | −1.9 | −2.1 | −1.3 | Yes | Histocompatibility 2, class II antigen A, beta 1 |
| H2-DMa | – | – | – | −1.6 | −1.6 | −1.0 | −1.1 | −1.4 | −1.5 | −0.9 | – | Histocompatibility 2, class II, locus DMa |
| H2-Eb1 | – | −1.4 | −1.8 | −2.2 | −2.2 | −1.0 | −1.2 | −1.7 | −1.7 | −1.0 | Yes | Histocompatibility 2, class II antigen E beta |
| H2-T23 | – | −1.4 | −1.5 | −1.4 | −1.2 | −0.9 | −1.1 | −1.0 | −1.1 | −0.8 | Yes | Histocompatibility 2, T region locus 23 |
| Irgm | – | – | −1.5 | −1.6 | −1.1 | −1.2 | −1.2 | −1.3 | −1.5 | −1.1 | - | Immunity-related GTPase family, M |
| Psmb10 | – | – | – | −1.3 | −1.3 | −1.0 | −0.9 | −1.2 | −1.2 | −0.8 | Yes | Proteasome (prosome, macropain) subunit, beta type, 10 |

Table 3 (*continued*)

| Gene symbol | Kidney cortex | | | | | Kidney medulla | | | | | Normal kidney tissue expression Gene expression[a] | |
|---|---|---|---|---|---|---|---|---|---|---|---|---|
| | 0.13 Gy | 0.34 Gy | 1.3 Gy | 4.3 Gy | 13 Gy | 0.13 Gy | 0.34 Gy | 1.3 Gy | 4.3 Gy | 13 Gy | Mouse | Description |
| Psmb8 | – | – | – | –1.0 | – | –0.7 | –0.8 | –1.0 | –1.0 | –0.7 | Yes | Proteasome (prosome, macropain) subunit, beta type, 8 (large multifunctional peptidase 7) |
| S100a8 | – | –1.6 | –1.8 | –1.3 | –1.4 | –0.8 | –1.6 | –1.7 | –1.5 | –1.5 | Yes | S100 calcium binding protein A8 |
| Socs3 | – | –1.1 | –1.1 | –1.1 | – | –1.4 | –1.5 | –1.4 | –1.4 | –1.0 | Yes | Suppressor of cytokine signaling 3 |
| Stat1 | – | – | – | –0.9 | – | –1.0 | –0.9 | –1.0 | –1.2 | –0.9 | Yes | Signal transducer and activator of transcription 1 |
| Ubd | – | – | –1.6 | –1.7 | –1.3 | –0.9 | –1.1 | –1.6 | –1.7 | –1.4 | – | Ubiquitin D |
| Avpr1a | – | – | – | – | –0.8 | –0.8 | –0.9 | –0.9 | –1.1 | –1.1 | Yes | Arginine vasopressin receptor 1A |
| Acaa1b | – | 1.0 | – | – | – | 1.0 | 1.1 | 0.9 | 1.0 | 0.8 | Yes | Acetyl-CoA acyltransferase 1 |
| Ak3l1 | – | 1.3 | – | 1.1 | – | 0.9 | 1.2 | 0.8 | 0.9 | 0.8 | NA | Adenylate kinase |
| Cml3 | – | 1.5 | – | – | 1.2 | 1.0 | 1.8 | 0.8 | 1.6 | 1.3 | Yes | Camello-like 3 |
| Dgat2 | – | – | 1.2 | 1.2 | – | 0.7 | 0.9 | 0.9 | 1.0 | 0.8 | Yes | Diacylglycerol O-acyltransferase 2 |

Gene symbols and gene expression log$_2$ ratios for the differentially expressed transcripts identified at all absorbed dose levels for kidney cortex and medulla. The normal expression of these genes in kidney tissue is presented according to Unigene. Red corresponds to down-regulation and green to up-regulation, and the intensity in color corresponds to the degree of regulation.

Explanation of denotation: Yes, mRNA levels found in normal tissue; NA, data not available; −, gene not found.

[a] Mouse gene expression data from Unigene.

processes such as glycolysis/gluconeogenesis and synthesis/degradation of ketone bodies, oxidative phosphorylation, Rho-mediated cell motility, and non-homologous end joining have been found affected by irradiation of specifically epithelial cells *in vitro* [34]. This diversity is also reflected by the results presented in this study, potentially related to genotoxic stress induced by the radiation exposure. However, single cell analysis comparing different cell types may separate the renal cell type response from other epithelial and vascular cell type response. Thus, the effects demonstrated in the present study represent the combined effects from all cells and cell types in the tissue analyzed.

Previously, gene expression profiles have been investigated and altogether 93 potential biomarkers for radiation exposure have been identified [22,30,35–37]. In our data set, only seven of these 93 genes were regulated in kidney cortex. These seven genes were regulated at the highest dose level (13 Gy), while 0, 0, 2, and 3 genes were regulated for the dose levels 0.13, 0.34, 1.3, and 4.3 Gy, respectively, with some genes regulated at more than one absorbed dose level. In kidney medulla, 12 of the 93 genes were found regulated with 1, 1, 6, 4, and 6 gene(s) regulated at the dose levels 0.13, 0.34, 1.3, 4.3, and 13 Gy, respectively. No genes were regulated at more than three dose levels and only two genes were regulated at three dose levels, both in kidney cortex and in medulla: *Ccng1* and *Cdkn1a*, both involved in regulation of cyclin-dependent protein and kinase activity. Furthermore, some genes have been proposed to be consistently regulated

**Table 4**
Gene Ontology enriched terms for transcripts with a log$_2$-ratio above 2.

| Tissue | Absorbed dose | Cell cycle and differentiation | Stress response | Cellular integrity | Metabolism | Gene expression integrity | Cell communication | Organismic regulation |
|---|---|---|---|---|---|---|---|---|
| Cortex | 0.13 Gy | | Angptl4 | Slc7a12 Ucp1 | Serpina10 Hmgcs2 | | | |
| | 0.34 Gy | | | | Hmgcs2 | | | |
| | 1.3 Gy | | H2-Ab1 Angptl4 | | Pck1 Cyp24a1 | | | |
| | 4.3 Gy | Phlda3 | H2-Ab1 H2-Ea H2-Eb1 Cd74 Igtp Gbp1 H2-DMb1 Angptl4 | | Serpina10 | | | |
| | 13 Gy | Ccng1 Cdkn1a Phlda3 | Ephx1 | Actg2 | | | | |
| Medulla | 0.13 Gy | | | Ucp1 | Hmgcs2 | | | |
| | 0.34 Gy | | Lcn2 | | Hmgcs2 | | | |
| | 1.3 Gy | | Igtp Cfd | | Pck1 Cyp24a1 Car3 | | | |
| | 4.3 Gy | | Igtp Lcn2 H2-Ab1 Scgb1a1 | | Igf2 | | | |
| | 13 Gy | Phlda3 Cdkn1a | | | | | | |

Differentially expressed transcripts with log$_2$-ratio ≥ 2, either positive or negative regulation for the different tissues, absorbed dose levels, and according to gene function.
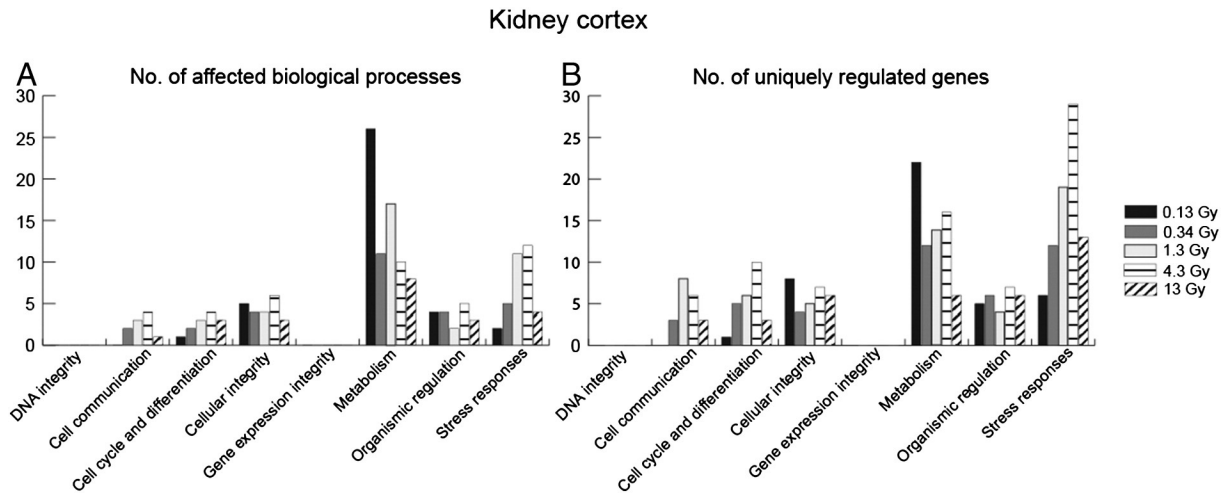
## Kidney cortex



**Fig. 1.** Affected biological processes and uniquely regulated transcripts in kidney cortex. Number of affected biological processes (A) for each absorbed dose in kidney cortex after injection of 1.3–140 MBq ^{177}Lu-octreotate categorized according to higher level cellular function. The number of uniquely regulated genes for each category per absorbed dose is shown in (B).

after both high and low absorbed doses. In the present study *Cdkn1a* was only regulated at 1.3 to 13 Gy, not at the lower absorbed doses. *Gadd45* (growth arrest and DNA-damage-inducible 45 beta), which has been found to be frequently regulated after radiation therapy [35], was not detected in our data sets, not even at the higher absorbed dose levels. These findings illustrate the differences in results obtained between different cell lines as well as between different tissue types, but also between *in vivo vs. in vitro* studies, since the proposed genes have predominantly been identified in *in vitro* studies.

Studies investigating whole transcriptional response following internal irradiation are few. Our group has previously found a strong association with metabolic processes after low dose ^{131}I and [211]At irradiation of the kidneys [22,23]. The present results strengthen the conclusion that irradiation of kidney tissue with low absorbed doses primarily has an impact on basal metabolic processes.

Other studies have investigated changes in gene expression patterns following acute or chronic external irradiation of the kidneys. Zhao and colleagues demonstrated the gene expression profiles of the kidneys 8 h and 24 h after 10 Gy ^{137}Cs whole body irradiation (4Gy/min) [21]. Although a lower number of genes were found regulated (42 genes), compared to the present study, the strongest response

involved genes were associated with transcription, translation, and metabolism. In the present study, few processes were associated with gene expression integrity, while a strong association with metabolism was found. However, no common genes associated with metabolism were detected by Zhao and colleagues and the present study. The discordance between the study from Zhao et al. and the present study can be due to several factors, such as differences in mouse strain, the type of irradiation (radionuclide, absorbed dose, dose rate, etc.), as well as differences in the microarray platforms. In this study, the Illumina whole transcriptome microarray platform was used, while the previous study used other platforms containing fewer probes, which might result in the detection of fewer regulated transcripts. Another very important difference is the potential systemic effects from other irradiated tissues [38], where whole body irradiation will give similar absorbed dose to all tissue types, while in the present study, non-kidney tissue types will receive a much lower absorbed dose than the kidneys, which increases the possibility of finding kidney-specific transcript regulation in the present study.

The dose–response relationship for a suitable single biomarker for toxicity is preferably a function with a monotone increase or decrease with absorbed dose. In the present investigation, few specific
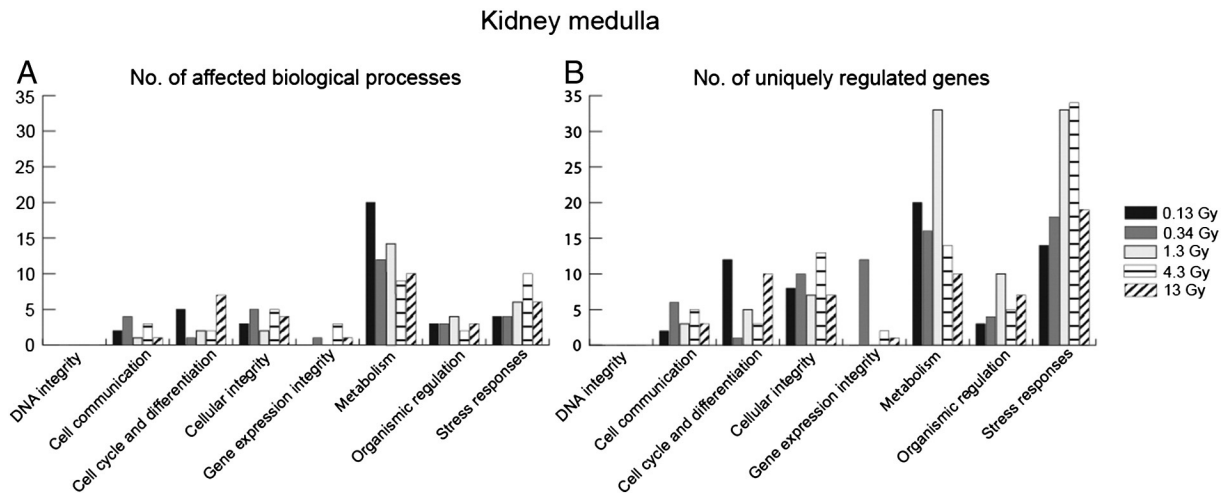
## Kidney medulla



**Fig. 2.** Affected biological processes and uniquely regulated transcripts in kidney medulla. Number of affected biological processes (A) for each absorbed dose in kidney medulla after injection of 1.3–140 MBq ^{177}Lu-octreotate categorized according to higher level cellular function. The number of uniquely regulated genes for each category per absorbed dose is shown in (B).

genes showed monotone increase or decrease in expression with increased absorbed dose. The majority of the affected transcripts revealed little or no difference in response between the different absorbed dose levels. The only exception was increasing down regulation of the expression of the *Hmgcs2* gene with increasing absorbed dose after an up-regulation at the lowest dose level studied. The *Havcr1* (hepatitis A virus cellular receptor 1) gene was differentially expressed at all absorbed doses in kidney cortex, and has previously been proposed as a predictor of kidney tubular damage, and its corresponding protein is measurable in urine [39,40]. However, genes that only show strong regulation at the higher absorbed doses may also prove to be a desired relationship. The *Cdkn1a* gene showed a strong increase in gene expression regulation in kidney cortex between the 4.3 ($log_2$-ratio 1.5) and 13 Gy ($log_2$-ratio 2.4) dose levels. Similar increase but with weaker regulation was found in kidney medulla. This gene has previously been proposed as biomarker for ionizing radiation as well as acute kidney injury [35,36,41]. The *Gdf15* gene also showed interesting expression with down-regulation at the lower absorbed doses (0.13 and 0.34 Gy) with subsequent increase in up-regulation with increasing absorbed dose for 1.3-13 Gy in both kidney cortex and medulla. However, the change in expression of this gene was only significant at the highest absorbed dose (13 Gy) for both tissues. This gene has also been proposed as a potential biomarker for kidney injury [41]. The regulation of the expression of these genes, and other with similar response, may also hold a desired dose–response relationship with the function of reflecting major risk for toxicity.

The regulation of expression of one specific gene may, however, not be adequate for the use as biomarker for kidney injury after radiation exposure, due to the complex response of the injury progression [42]. Rather, the expression pattern of several genes may prove to be more useful, where the expression of certain genes at specific absorbed dose levels, as well as time, should be considered in more detail. This type of analysis will be performed when more data has been obtained.

To our knowledge, none of the genes which demonstrate significantly regulated expression at all absorbed doses in the present study have previously been proposed as a biomarker for kidney response to radiation. However, in mice 24 h after $^{131}$I administration, the *Cyp24a1* (Cytochrome P450) gene expression was up-regulated whereas the *Serpina10* (Serpin peptidase inhibitor) and the *Havcr1* (hepatitis A virus cellular receptor 1) gene expressions were down-regulated at all absorbed doses in kidney cortex studied (0.17–3.5 mGy) [22]. Furthermore, in mice 24 h after $^{211}$At administration, the *Angptl4* (Angiopoietin-like 4) gene expression was up-regulated at all absorbed doses in both kidney cortex and medulla (0.24–160 mGy) [23]. Thus, indications of similar responses after administration of different radionuclides *in vivo* exist. However, a deeper analysis of the combined results of these studies is needed in order to draw any firm conclusions regarding the similarities and differences due to different radiation types.

## 5. Conclusion

The use of $^{177}$Lu-octreotate treatment of neuroendocrine tumors is rapidly rising. Due to the low cure rate and that kidneys is the main dose-limiting organ, more information on the molecular pathways and biological processes associated with kidney response to ionizing radiation is needed, information that is of great importance in the search of clinically useful biomarkers in preferably urine or blood. This study demonstrates distinct differences in the biological response obtained after different absorbed doses. However, the impact of these biological responses over longer time periods is still unknown. Therefore, further research is needed to evaluate late biological effects and correlate these to the risk of long-term or chronic side effects after $^{177}$Lu-octreotate treatment, as one of several steps towards patient-specific treatment.

Supplementary data to this article can be found online at http://dx.doi.org/10.1016/j.nucmedbio.2013.12.001.

## References

[1] Khan S, Krenning EP, van Essen M, Kam BL, Teunissen JJ, Kwekkeboom DJ. Quality of life in 265 patients with gastroenteropancreatic or bronchial neuroendocrine tumors treated with [$^{177}$Lu-DOTA0, Tyr³]octreotate. J Nucl Med 2011;52:1361–8.

[2] Sward C, Bernhardt P, Ahlman H, Wangberg B, Forssell-Aronsson E, Larsson M, et al. [$^{177}$Lu-DOTA 0-Tyr³]-octreotate treatment in patients with disseminated gastroenteropancreatic neuroendocrine tumors: the value of measuring absorbed dose to the kidney. World J Surg 2010;34:1368–72.

[3] Forssell-Aronsson E, Bernhardt P, Nilsson O, Tisell LE, Wangberg B, Ahlman H. Biodistribution data from 100 patients i.v. injected with $^{111}$In-DTPA-D-Phe¹-octreotide. Acta Oncol 2004;43:436–42.

[4] Forssell-Aronsson E, Nilsson O, Benjegard SA, Kolby L, Bernhardt P, Molne J, et al. $^{111}$In-DTPA-D-Phe¹-octreotide binding and somatostatin receptor subtypes in thyroid tumors. J Nucl Med 2000;41:636–42.

[5] de Jong M, Rolleman EJ, Bernard BF, Visser TJ, Bakker WH, Breeman WA, et al. Inhibition of renal uptake of indium-111-DTPA-octreotide in vivo. J Nucl Med 1996;37:1388–92.

[6] Christensen EI, Nielsen S. Structural and functional features of protein handling in the kidney proximal tubule. Semin Nephrol 1991;11:414–39.

[7] Vegt E, de Jong M, Wetzels JF, Masereeuw R, Melis M, Oyen WJ, et al. Renal toxicity of radiolabeled peptides and antibody fragments: mechanisms, impact on radionuclide therapy, and strategies for prevention. J Nucl Med 2010;51:1049–58.

[8] Forssell-Aronsson E, Spetz J, Ahlman H. Radionuclide therapy via SSTR: future aspects from experimental animal studies. Neuroendocrinology 2013;97:86–98.

[9] Kolby L, Bernhardt P, Johanson V, Schmitt A, Ahlman H, Forssell-Aronsson E, et al. Successful receptor-mediated radiation therapy of xenografted human midgut carcinoid tumour. Br J Cancer 2005;93:1144–51.

[10] Dalmo J, Rudqvist N, Spetz J, Laverman P, Nilsson O, Ahlman H, et al. Biodistribution of $^{177}$Lu-octreotide and $^{111}$In-minigastrin in female nude mice transplanted with human medullary thyroid carcinoma GOT2. Oncol Rep 2012;27:174–81.

[11] Larsson M, Bernhardt P, Svensson JB, Wangberg B, Ahlman H, Forssell-Aronsson E. Estimation of absorbed dose to the kidneys in patients after treatment with $^{177}$Lu-octreotate: comparison between methods based on planar scintigraphy. EJNMMI Res 2012;2:49.

[12] Valkema R, Pauwels SA, Kvols LK, Kwekkeboom DJ, Jamar F, de Jong M, et al. Long-term follow-up of renal function after peptide receptor radiation therapy with $^{90}$Y-DOTA⁰, Tyr³-octreotide and $^{177}$Lu-DOTA⁰, Tyr³-octreotate. J Nucl Med 2005;46(Suppl 1):83S–91S.

[13] Emami B, Lyman J, Brown A, Coia L, Goitein M, Munzenrider JE, et al. Tolerance of normal tissue to therapeutic irradiation. Int J Radiat Oncol Biol Phys 1991;21:109–22.

[14] Lambert B, Cybulla M, Weiner SM, Van De Wiele C, Ham H, Dierckx RA, et al. Renal toxicity after radionuclide therapy. Radiat Res 2004;161:607–11.

[15] Svensson J, Molne J, Forssell-Aronsson E, Konijnenberg M, Bernhardt P. Nephrotoxicity profiles and threshold dose values for [$^{177}$Lu]-DOTATATE in nude mice. Nucl Med Biol 2012;39:756–62.

[16] Cybulla M, Weiner SM, Otte A. End-stage renal disease after treatment with $^{90}$Y-DOTATOC. Eur J Nucl Med 2001;28:1552–4.

[17] Otte A, Herrmann R, Heppeler A, Behe M, Jermann E, Powell P, et al. Yttrium-90 DOTATOC: first clinical results. Eur J Nucl Med 1999;26:1439–47.

[18] Pool SE, Krenning EP, Koning GA, van Eijck CH, Teunissen JJ, Kam B, et al. Preclinical and clinical studies of peptide receptor radionuclide therapy. Semin Nucl Med 2010;40:209–18.

[19] Kruse JJ, te Poele JA, Velds A, Kerkhoven RM, Boersma LJ, Russell NS, et al. Identification of differentially expressed genes in mouse kidney after irradiation using microarray analysis. Radiat Res 2004;161:28–38.

[20] Taki K, Wang B, Nakajima T, Wu J, Ono T, Uehara Y, et al. Microarray analysis of differentially expressed genes in the kidneys and testes of mice after long-term irradiation with low-dose-rate gamma-rays. J Radiat Res (Tokyo) 2009;50:241–52.

[21] Zhao W, Chuang EY, Mishra M, Awwad R, Bisht K, Sun L, et al. Distinct effects of ionizing radiation on in vivo murine kidney and brain normal tissue gene expression. Clin Cancer Res 2006;12:3823–30.

[22] Schuler E, Parris TZ, Rudqvist N, Helou K, Forssell-Aronsson E. Effects of internal low-dose irradiation from $^{131}$I on gene expression in normal tissues in Balb/c mice. EJNMMI Res 2011;1:29.

[23] Langen B, Rudqvist N, Parris TZ, Schüler E, Helou K, Forssell-Aronsson E. Comparative analysis of transcriptional gene regulation indicates similar physiologic response in mouse tissues at low absorbed doses from intravenously administered $^{211}$At. J Nucl Med 2013;54:990–8.

[24] Loevinger R, Budinger TF, Watson EE. MIRD primer for absorbed dose calculations. Society of Nuclear Medicine; 1988.

[25] Miller WH, Hartmann-Siantar C, Fisher D, Descalle MA, Daly T, Lehmann J, et al. Evaluation of beta-absorbed fractions in a mouse model for $^{90}$Y, $^{188}$Re, $^{166}$Ho, $^{149}$Pm, $^{64}$Cu, and $^{177}$Lu radionuclides. Cancer Biother Radiopharm 2005;20: 436–49.

[26] Benjamini Y, Hochberg Y. Controlling the false discovery rate: a practical and powerful approach to multiple testing. J R Stat Soc B 1995;57:289–300.

[27] Melis M, Krenning EP, Bernard BF, Barone R, Visser TJ, de Jong M. Localisation and mechanism of renal retention of radiolabelled somatostatin analogues. Eur J Nucl Med Mol Imaging 2005;32:1136–43.

[28] De Jong M, Valkema R, Van Gameren A, Van Boven H, Bex A, Van De Weyer EP, et al. Inhomogeneous localization of radioactivity in the human kidney after injection of [$^{111}$In-DTPA]octreotide. J Nucl Med 2004;45:1168–71.

[29] Konijnenberg M, Melis M, Valkema R, Krenning E, de Jong M. Radiation dose distribution in human kidneys by octreotides in peptide receptor radionuclide therapy. J Nucl Med 2007;48:134–42.

[30] Rudqvist N, Parris TZ, Schuler E, Helou K, Forssell-Aronsson E. Transcriptional response of BALB/c mouse thyroids following in vivo astatine-211 exposure reveals distinct gene expression profiles. EJNMMI Res 2012;2:32.

[31] Heinloth AN, Shackelford RE, Innes CL, Bennett L, Li L, Amin RP, et al. ATM-dependent and -independent gene expression changes in response to oxidative stress, gamma irradiation, and UV irradiation. Radiat Res 2003;160:273–90.

[32] Heinloth AN, Shackelford RE, Innes CL, Bennett L, Li L, Amin RP, et al. Identification of distinct and common gene expression changes after oxidative stress and gamma and ultraviolet radiation. Mol Carcinog 2003;37:65–82.

[33] Rashi-Elkeles S, Elkon R, Shavit S, Lerenthal Y, Linhart C, Kupershtein A, et al. Transcriptional modulation induced by ionizing radiation: p53 remains a central player. Mol Oncol 2011;5:336–48.

[34] Sriharshan A, Boldt K, Sarioglu H, Barjaktarovic Z, Azimzadeh O, Hieber L, et al. Proteomic analysis by SILAC and 2D-DIGE reveals radiation-induced endothelial response: four key pathways. J Proteomics 2012;75:2319–30.

[35] Snyder AR, Morgan WF. Gene expression profiling after irradiation: clues to understanding acute and persistent responses? Cancer Metastasis Rev 2004;23: 259–68.

[36] Chaudhry MA. Biomarkers for human radiation exposure. J Biomed Sci 2008;15: 557–63.

[37] Filiano AN, Fathallah-Shaykh HM, Fiveash J, Gage J, Cantor A, Kharbanda S, et al. Gene expression analysis in radiotherapy patients and C57BL/6 mice as a measure of exposure to ionizing radiation. Radiat Res 2011;176:49–61.

[38] Langen B. Fundamental studies on high-LET radiation induced DNA damage in vitro and transcriptional responses in vivo. Licentiate thesis, Department of Applied Physics: Chalmers University of Technology, Gothenburg, Sweden; 2013.

[39] Vaidya VS, Ozer JS, Dieterle F, Collings FB, Ramirez V, Troth S, et al. Kidney injury molecule-1 outperforms traditional biomarkers of kidney injury in preclinical biomarker qualification studies. Nat Biotechnol 2010;28:478–85.

[40] Han WK, Bailly V, Abichandani R, Thadhani R, Bonventre JV. Kidney injury molecule-1 (KIM-1): a novel biomarker for human renal proximal tubule injury. Kidney Int 2002;62:237–44.

[41] Vaidya VS, Ferguson MA, Bonventre JV. Biomarkers of acute kidney injury. Annu Rev Pharmacol Toxicol 2008;48:463–93.

[42] Adiyanti SS, Loho T. Acute kidney injury (AKI) biomarker. Acta Med Indones 2012;44:246–55.